Hindawi Publishing Corporation
Mathematical Problems in Engineering
Volume 2015, Article ID 686857, 8 pages
http://dx.doi.org/10.1155/2015/686857

Research Article

$\mathcal{H}_\infty$ LPV Control with Pole Placement Constraints for Synchronous Buck Converters with Piecewise-Constant Loads

Hwanyub Joo and Sung Hyun Kim

School of Electrical Engineering, University of Ulsan (UOU), Ulsan 680-749, Republic of Korea

Correspondence should be addressed to Sung Hyun Kim; shnkim@ulsan.ac.kr

Received 5 June 2014; Revised 12 August 2014; Accepted 26 August 2014

Academic Editor: Guido Maione

This paper addresses the output regulation problem of synchronous buck converters with piecewise-constant load fluctuations via linear parameter varying (LPV) control scheme. To this end, an output-error state-space model is first derived in the form of LPV systems so that it can involve a mismatch error that temporally arises from the process of generating a feedforward control. Then, to attenuate the mismatch error in parallel with improving the transient behavior of the converter, this paper proposes an LMI-based stabilization condition capable of achieving both $\mathcal{H}_\infty$ and pole-placement objectives. Finally, the simulation and experimental results are provided to show the validity of our approach.

1. Introduction

Drawing on the development of electronic technology, switching DC-DC converters have been widely and successfully applied to a variety of power conversion systems such as DC power supplies, DC motor drivers, and power generation systems (see [1–4] and the references therein). Recently, with the growing interest in linear matrix inequalities (LMIs) [5], some advanced control techniques have been investigated regarding to output regulation of DC-DC buck (step-down) converters that produce a lower output voltage than the input voltage, especially for T-S fuzzy control [2, 6–10]. Indeed, the asynchronous buck converters operating in a large-signal domain are generally modeled in terms of nonlinear systems. Thus, based on the T-S fuzzy model derived from the averaging method for one-time-scale discontinuous systems (AM-OTS-DS), [9] has successfully designed an integral T-S fuzzy control with respect to the output regulation problem of the asynchronous buck converter. Meanwhile, in the case of synchronous buck converters [11–13], the use of the low-side FET plays an important role in eliminating the voltage drop across the power diode of the nonsynchronous converter, which allows buck converters to be modeled with linear time-varying systems.

In general, the operation of the DC-DC converter is usually affected by the fluctuation of output loads [3, 9, 12, 13]. For this reason, it is of great importance to consider the presence of a wide load range in the problem of regulating the output voltage and current levels of DC-DC converters; that is, it has become a hot topic to maintain high efficiency in a great load fluctuation. Moreover, due to the fact that conventional pulse-width modulation (PWM) buck converters have poor efficiency under light load [14], numerous research efforts have been invested to improve the efficiency of the PWM converters with a wide load range (see [12, 15–17] and the references therein). However, a remarkable point is that most of references cited above have paid considerable attention at the hardware level to cover such problem. Further, [13] used a reduced system model with the limits in theoretically capturing the dynamic behavior of piecewise-constant load fluctuation in the process of implementing the robust periodic eigenvalue assignment algorithm [18]. In other words, limited work has been found in terms of the control theory. Motivated by the concern, this paper proposes a suitable approach in light of the control theory to take the effect of load fluctuations into account.

This paper addresses the output regulation problem of synchronous buck converters with piecewise-constant load

fluctuations. To consider the presence of such load fluctuations, we derive an output-error state-space model in the form of linear parameter varying (LPV) systems [19–21], thereby converting the underlying regulation problem into the stabilization problem. Here, it is worth noticing that a mismatch error that temporally arises from the process of generating a feedforward control is clearly incorporated into the LPV model and it is attenuated by the $\mathscr{H}_\infty$-synthesis technique [22, 23]. However, $\mathscr{H}_\infty$ design provides little control over the transient behavior [24, 25]. Hence, to attenuate the mismatch error in parallel with improving the transient behavior of the converter, this paper proposes an LMI-based stabilization condition capable of achieving both $\mathscr{H}_\infty$ and pole-placement objectives. Finally, the simulation and experimental results are provided to show the validity of our approach.

Notation. The notations $X \geq Y$ and $X > Y$ mean that $X - Y$ is positive semidefinite and positive definite, respectively. In symmetric block matrices, $(*)$ is used as an ellipsis for terms induced by symmetry. For any square matrix $\mathcal{Q}$, $\mathbf{He}[\mathcal{Q}] = \mathcal{Q} + \mathcal{Q}^T$. Lebesgue space $\mathscr{L}_{2+} = \mathscr{L}_2[0, \infty)$ consists of square-integrable functions on $[0, \infty)$.

2. Modeling for DC to DC PWM Buck Converter

The equivalent circuit for a class of synchronous DC-DC buck converters and the corresponding closed-loop control system are depicted in Figure 1, where the following notations are used.

(i) R_{DS} denotes the static drain to source resistances of the high-side and low-side power MOSFETs, respectively.

(ii) $v_I(t)$ and $v_O(t)$ denote the power input and output voltages, respectively, where it is assumed that $v_I(t) = v_I$ is time-invariant.

(iii) $i_L(t)$ and $v_C(t)$ denote the inductor current and the capacitor voltage, respectively.

(iv) L and C denote the inductance and capacitance selected by the given design specifications including the switching frequency of MOSFETs.

(v) R_{DCR} and R_{ESR} denote the equivalent series resistances of the inductor and capacitor.

(vi) $R(t)$ and $\tau(t)$ denote the piecewise-constant load resistance subject to $R^- \leq R(t) \leq R^+$ and the duty ratio of PWM buck converter.

Then, based on averaging method for one-time-scale discontinuous system (AM-OTS-DS) [26], the mathematical model of the buck converter under consideration is described as follows:

$$\dot{i}_L(t) = -\frac{1}{L} v_O(t) - \frac{R_{\mathrm{DS}} + R_{\mathrm{DCR}}}{L} i_L(t) + \frac{1}{L} v_I \tau(t), \quad (1)$$

$$\dot{v}_C(t) = \frac{1}{C} i_L(t) - \frac{1}{R(t)C} v_O(t), \quad (2)$$

$$\dot{v}_C(t) = \frac{1}{R_{\mathrm{ESR}}C} \left(v_O(t) - v_C(t)\right). \quad (3)$$

Further, combining (2) and (3) yields

$$v_O(t) = \frac{R(t)}{R(t) + R_{\mathrm{ESR}}} \left(R_{\mathrm{ESR}} i_L(t) + v_C(t)\right), \quad (4)$$

by which (1) and (2) can be rewritten as follows:

$$\begin{aligned} \dot{i}_L(t) = &-\frac{1}{L}\left(\frac{R(t)R_{\mathrm{ESR}}}{R(t) + R_{\mathrm{ESR}}} + R_{\mathrm{DS}} + R_{\mathrm{DCR}}\right) i_L(t) \\ &- \frac{1}{L}\frac{R(t)}{R(t) + R_{\mathrm{ESR}}} v_C(t) + \frac{v_I}{L}\tau(t), \end{aligned} \quad (5)$$

$$\begin{aligned} \dot{v}_C(t) = &\frac{1}{C}\frac{R(t)}{R(t) + R_{\mathrm{ESR}}} i_L(t) \\ &- \frac{1}{C}\frac{1}{R(t) + R_{\mathrm{ESR}}} v_C(t). \end{aligned} \quad (6)$$

Let $\bar{v}_C$ be a unique equilibrium point of $v_C(t)$ and assume that the value of $R(t)$ is piecewise-constant; that is, $R(t) = R_j$ for $t \in \mathscr{T}_j$ (see Figure 1). Then, by (6), the equilibrium point of $i_L(t)$, that is, $\bar{i}_L$, is given by

$$0 = R_j \bar{i}_L - \bar{v}_C, \quad \text{for } t \in \mathscr{T}_j. \quad (7)$$

Further, by (3), the equilibrium point of $v_O(t)$ is given by $\bar{v}_O = \bar{v}_C$. Hence, from (1), the equilibrium point of $\tau(t)$, that is, $\bar{\tau}$, is given by

$$0 = \bar{v}_C + \left(R_{\mathrm{DS}} + R_{\mathrm{DCR}}\right)\bar{i}_L - v_I \bar{\tau}, \quad \text{for } t \in \mathscr{T}_j. \quad (8)$$

Remark 1. This paper focuses on addressing the case where the variation of $R(t)$ is subject to a class of switching signals whose finite intervals $\mathscr{T}_j$ are larger than the setting time.

Remark 2. Indeed, it is extremely hard to directly measure the value of $v_C(t)$ in the considered buck converter owing to the existence of R_{ESR} (see Figure 1). Thus, to find the value of $v_C(t)$ from the ones of the measured $v_O(t)$, $i_O(t)$, and $i_L(t)$, we introduce a method of using the following equality derived from (4):

$$v_C(t) = v_O(t) + R_{\mathrm{ESR}}\left(i_O(t) - i_L(t)\right). \quad (9)$$

Remark 3. From (9), we can see that $\bar{i}_O = \bar{i}_L$ in the equilibrium point, because $\bar{v}_C = \bar{v}_O$.

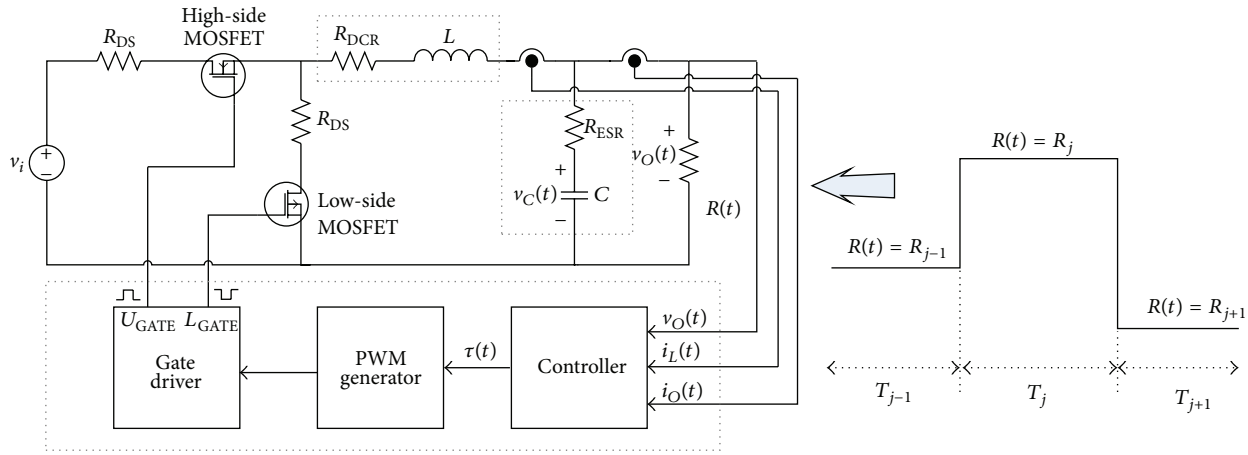

Figure 1: Equivalent circuit for a class of synchronous DC-DC buck converters and piecewise-constant load fluctuations.

Remark 4. To solve the regulation problem herein, we need to find the desired value of $\bar{i}_L = \bar{v}_C/R_j$ from (7), where $\bar{v}_C$ is a prescribed value and R_j can be established as follows:

$$R_j = \begin{cases} R^-, & \text{if } \dfrac{v_O(t)}{i_O(t)} < R^- \\ R^+, & \text{if } \dfrac{v_O(t)}{i_O(t)} > R^+ \\ \dfrac{v_O(t)}{i_O(t)}, & \text{otherwise.} \end{cases} \tag{10}$$

3. LPV Control with Pole Placement Constraints

3.1. LPV Model Description. Let $\tilde{i}_L(t) = i_L(t) - \bar{i}_L$, $\tilde{v}_C(t) = v_C(t) - \bar{v}_C$, and $\tau(t) = u(t) + \psi(t)$, where $u(t)$ and $\psi(t)$ indicate the feedback and feedforward control inputs, respectively. Then, for $t \in \mathcal{T}_j$, the system given in (5) and (6) can be converted into

$$\begin{aligned} \dot{\tilde{i}}_L(t) &= -\frac{1}{L}\left(\frac{R_j R_{\mathrm{ESR}}}{R_j + R_{\mathrm{ESR}}} + R_{\mathrm{DS}} + R_{\mathrm{DCR}}\right)\tilde{i}_L(t) \\ &\quad - \frac{1}{L}\frac{R_j}{R_j + R_{\mathrm{ESR}}}\tilde{v}_C(t) + \frac{v_I}{L}u(t) \\ &\quad - \frac{1}{L}\left(\frac{R_j R_{\mathrm{ESR}}}{R_j + R_{\mathrm{ESR}}} + R_{\mathrm{DS}} + R_{\mathrm{DCR}}\right)\bar{i}_L \\ &\quad - \frac{1}{L}\frac{R_j}{R_j + R_{\mathrm{ESR}}}\bar{v}_C + \frac{v_I}{L}\psi(t), \\ \dot{\tilde{v}}_C(t) &= \frac{1}{C}\frac{R_j}{R_j + R_{\mathrm{ESR}}}\tilde{i}_L(t) - \frac{1}{C}\frac{1}{R_j + R_{\mathrm{ESR}}}\tilde{v}_C(t) \\ &\quad + \frac{1}{C}\frac{1}{R_j + R_{\mathrm{ESR}}}\left(R_j\bar{i}_L - \bar{v}_C\right). \end{aligned} \tag{11}$$

Proposition 5. *Let us consider the feedforward control input $\psi(t)$ of the following form:*

$$\begin{aligned} \psi(t) &= \frac{1}{v_I}\left(\left(\frac{R_j R_{ESR}}{R_j + R_{ESR}} + R_{DS} + R_{DCR}\right)\bar{i}_L \right. \\ &\qquad \left. + \frac{R_j}{R_j + R_{ESR}}\bar{v}_C\right) + w(t) \\ &= \frac{1}{v_I}\left(\bar{v}_C + \left(R_{DS} + R_{DCR}\right)\bar{i}_L\right) + w(t) \\ &= \bar{\tau} + w(t), \end{aligned} \tag{12}$$

where $w(t) \in \mathcal{L}_{2+}$ denotes the error that can temporally occur when finding R_j and $\bar{i}_{L,j}$ under the saturation operator (10). Here, a remarkable point is that if $w(t) = 0$, then the feedforward control input $\psi(t) = \bar{\tau}$ for $t \in \mathcal{T}_j$.

Under (12), the system given in (11) becomes

$$\begin{aligned} \dot{\tilde{i}}_L(t) &= -\frac{1}{L}\left(\frac{R_j R_{\mathrm{ESR}}}{R_j + R_{\mathrm{ESR}}} + R_{\mathrm{DS}} + R_{\mathrm{DCR}}\right)\tilde{i}_L(t) \\ &\quad - \frac{1}{L}\frac{R_j}{R_j + R_{\mathrm{ESR}}}\tilde{v}_C(t) + \frac{v_I}{L}u(t) + \frac{v_I}{L}w(t), \\ \dot{\tilde{v}}_C(t) &= \frac{1}{C}\frac{R_j}{R_j + R_{\mathrm{ESR}}}\tilde{i}_L(t) \\ &\quad - \frac{1}{C}\frac{1}{R_j + R_{\mathrm{ESR}}}\tilde{v}_C(t), \quad \text{for } t \in \mathcal{T}_j. \end{aligned} \tag{13}$$

In what follows, let us define

$$f_1 = \frac{R_j}{R_j + R_{\mathrm{ESR}}}, \quad f_2 = \frac{1}{R_j + R_{\mathrm{ESR}}}, \quad \forall j. \tag{14}$$

Then, by letting $x(t) = \mathbf{col}(\tilde{i}_L(t), \tilde{v}_C(t))$, we can rewrite (13) as follows:

$$\dot{x}(t) = A\left(f_1, f_2\right)x(t) + B_u u(t) + B_w w(t), \tag{15}$$

where

$$A(f_1, f_2) = \begin{bmatrix} -\frac{1}{L}\left(R_{\mathrm{ESR}} f_1 + R_{\mathrm{DS}} + R_{\mathrm{DCR}}\right) & -\frac{1}{L} f_1 \\ \frac{1}{C} f_1 & -\frac{1}{C} f_2 \end{bmatrix}, \quad B_u = B_w = \begin{bmatrix} \frac{v_I}{L} \\ 0 \end{bmatrix}. \tag{16}$$

Here, note that, from the fact that

$$0 < f_{1,0} = \frac{R^-}{R^- + R_{\mathrm{ESR}}} \le f_1 \le \frac{R^+}{R^+ + R_{\mathrm{ESR}}} = f_{1,1}, \quad 0 < f_{2,0} = \frac{1}{R^+ + R_{\mathrm{ESR}}} \le f_2 \le \frac{1}{R^- + R_{\mathrm{ESR}}} = f_{2,1}, \tag{17}$$

(14) can be represented by $f_1 = \sum_{i=0}^{1} \rho_{1,i} f_{1,i}$ and $f_2 = \sum_{i=0}^{1} \rho_{2,i} f_{2,i}$, where

$$\rho_{1,0} = \frac{f_{1,1} - f_1}{f_{1,1} - f_{1,0}}, \quad \rho_{1,1} = \frac{f_1 - f_{1,0}}{f_{1,1} - f_{1,0}}, \quad \rho_{2,0} = \frac{f_{2,1} - f_2}{f_{2,1} - f_{2,0}}, \quad \rho_{2,1} = \frac{f_2 - f_{2,0}}{f_{2,1} - f_{2,0}}. \tag{18}$$

Therefore, we can derive the linear parameter varying (LPV) form of $A(f_1, f_2)$ as follows:

$$A(f_1, f_2) = \sum_{p=1}^{4} \sigma_p A_p \triangleq A(\sigma), \quad \sigma_p = \rho_{1,[p]_1} \cdot \rho_{2,[p]_2}, \quad A_p = \begin{bmatrix} -\frac{1}{L}\left(R_{\mathrm{ESR}} f_{1,[p]_1} + R_{\mathrm{DS}} + R_{\mathrm{DCR}}\right) & -\frac{1}{L} f_{1,[p]_1} \\ \frac{1}{C} f_{1,[p]_1} & -\frac{1}{C} f_{2,[p]_2} \end{bmatrix}, \tag{19}$$

where $[p]_1$ and $[p]_2$ are decided from $p = 2[p]_2 + [p]_1 + 1$ and $[p]_k \in \{0, 1\}$. Here, it should be pointed out that the piecewise-constant parameters σ_p satisfy the following properties:

$$\sum_{p=1}^{4} \sigma_p = \sum_{[p]_1=0}^{1} \sum_{[p]_2=0}^{1} \rho_{1,[p]_1} \cdot \rho_{2,[p]_2} = \left(\sum_{[p]_1=0}^{1} \rho_{1,[p]_1} \right) \cdot \left(\sum_{[p]_2=0}^{1} \rho_{2,[p]_2} \right) = 1, \quad 0 \le \sigma_p \le 1, \quad \forall p. \tag{20}$$

3.2. Control Design. Now, consider a state-feedback control law of the following form:

$$u(t) = F(\sigma)\, x(t), \tag{21}$$

where $F(\sigma) = \sum_{p=1}^{4} \sigma_p F_p$. Then, the closed-loop system under (15) and (21) is given by

$$\dot{x}(t) = \left(A(\sigma) + B_u F(\sigma)\right) x(t) + B_w w(t), \tag{22}$$

$$z(t) = C_z x(t), \tag{23}$$

where $z(t)$ denotes the performance output in the $\mathscr{H}_\infty$ sense.

In order to address the $\mathscr{D}$-stability problem, we consider the following theorem reported in [24], which will be used for the design of LPV control with pole placement constraints.

Theorem 6 (see [24]). *The system matrix A is $\mathscr{D}$-stable (i.e., all the poles of A lie in $\mathscr{D}$) if and only if there exists a symmetric matrix X such that $M_{\mathscr{D}}(A, X) < 0$, $X > 0$, where $M_{\mathscr{D}}(A, X)$ is related with the following characteristic function $f_{\mathscr{D}}(z)$ on the basis of the substitution $(X, AX, XA^T) \rightleftharpoons (1, z, \overline{z})$:*

(i) *left half-plane such that $R(z) < -\alpha$: $\mathscr{D} = \{z \in \mathbf{C} \mid f_{\mathscr{D}}(z) = z + \overline{z} + 2\alpha < 0\}$,*

(ii) *disk with center at $(-q, 0)$ and radius r:*

$$\mathscr{D} = \left\{ z \in \mathbf{C} \mid f_{\mathscr{D}}(z) = \begin{bmatrix} -r & q + z \\ q + \overline{z} & -r \end{bmatrix} < 0 \right\}, \tag{24}$$

(iii) *conic sector centered at the origin and with inner angle 2θ:*

$$\mathscr{D} = \left\{ z \in \mathbf{C} \mid f_{\mathscr{D}}(z) = \begin{bmatrix} \sin\theta\,(z + \overline{z}) & \cos\theta\,(z - \overline{z}) \\ \cos\theta\,(z - \overline{z}) & \sin\theta\,(z + \overline{z}) \end{bmatrix} < 0 \right\}. \tag{25}$$

The following theorem presents a set of LMIs for $\mathscr{D}$-stability criterion for (22).

Theorem 7. *Let the required LMI region $\mathscr{D}$ be given in terms of α, r, θ, and $q = 0$. Then, (22) is $\mathscr{D}$-stable if there exist matrices $\{\overline{F}_p\}_{p=1,2,3,4} \in \mathbb{R}^{1\times 2}$ and symmetric matrix $0 < X \in \mathbb{R}^{2\times 2}$ such that, for all $p \in \{1, 2, 3, 4\}$,*

$$0 > \mathbf{He}\left[A_p X + B_u \overline{F}_p + \alpha X\right], \tag{26}$$

$$0 > \begin{bmatrix} -rX & A_p X + B_u \overline{F}_p \\ (*) & -rX \end{bmatrix}, \tag{27}$$

$$0 > \begin{bmatrix} \sin\theta \cdot \mathbf{He}\left[A_p X + B_u \overline{F}_p\right] \\ \cos\theta \cdot \left(A_p X + B_u \overline{F}_p - X A_p^T - \overline{F}_p^T B_u^T\right) \\ (*) \\ \sin\theta \cdot \mathbf{He}\left[A_p X + B_u \overline{F}_p\right] \end{bmatrix}, \tag{28}$$

$$0 > \begin{bmatrix} -I & C_z X & 0 \\ (*) & \mathbf{He}\left[A_p X + B_u \overline{F}_p\right] & B_w \\ (*) & (*) & -\gamma^2 I \end{bmatrix}. \tag{29}$$

Moreover, the control gains F_p can be reconstructed by $F_p = \overline{F}_p X^{-1}$.

Proof. From Theorem 6, the pole placement constraints are satisfied if and only if there exists $X > 0$ such that

$$M_D\left(A(\sigma) + B_u F(\sigma), X\right) < 0. \tag{30}$$

Accordingly, the $\mathscr{D}$-stability conditions of (22) are given by

$$\begin{aligned} 0 &> \mathbf{He}\left[\Phi(\sigma) + \alpha X\right], \\ 0 &> \begin{bmatrix} -rX & \Phi(\sigma) \\ (*) & -rX \end{bmatrix}, \\ 0 &> \begin{bmatrix} \sin\theta \cdot \mathbf{He}\left[\Phi(\sigma)\right] & \cos\theta \cdot \left(\Phi(\sigma) - \Phi(\sigma)^T\right) \\ (*) & \sin\theta \cdot \left(\mathbf{He}\left[\Phi(\sigma)\right]\right) \end{bmatrix}, \end{aligned} \tag{31}$$

where $\Phi(\sigma) = A(\sigma)X + B_u\overline{F}(\sigma)$ and $\overline{F}(\sigma) = F(\sigma)X = \sum_{p=1}^{4}\sigma_p F_p X$. By defining $\overline{F}_p = F_p X$, we can express that $\Phi(\sigma) = \sum_{p=1}^{4}\sigma_p(A_p X + B_u\overline{F}_p)$, which leads to $\Phi(\sigma) \in \mathbf{Co}(A_p X + B_u\overline{F}_p)$ by (20), where $\mathbf{Co}(\cdot)$ indicates the convex hull. Hence, the $\mathscr{D}$-stability conditions given in (31) can be assured by (26)–(28), respectively.

Next, we discuss the $\mathscr{H}_\infty$ performance such that $\mathbf{sup}_w(\|z(t)\|_2/\|w(t)\|_2) < \gamma$ for all $0 \neq w(t) \in \mathscr{L}_{2+}$, where γ represents the disturbance attenuation capability. As is well known, the $\mathscr{H}_\infty$ stability criterion [19] can be derived from

$$0 > z^T(t)z(t) - \gamma^2 w^T(t)w(t) + \dot{V}(t). \tag{32}$$

Here, let $V(t) = x^T(t)X^{-1}x(t)$. Then, (32) can be naturally rewritten as follows:

$$\begin{aligned} 0 > \mathbf{He}\left[x^T(t)X^{-1}\left(\left(A(\sigma) + B_u F(\sigma)\right)x(t) + B_w w(t)\right)\right] \\ + z^T(t)z(t) - \gamma^2 w^T(t)w(t), \end{aligned} \tag{33}$$

which leads to

$$0 > \begin{bmatrix} \mathbf{He}\left[X^{-1}\left(A(\sigma) + B_u F(\sigma)\right)\right] + C_z^T C_z & X^{-1}B_w \\ (*) & -\gamma^2 I \end{bmatrix}. \tag{34}$$

As a result, pre- and postmultiplying (34) by $\mathbf{diag}(X, I)$ and its transpose yield

$$0 > \begin{bmatrix} \mathbf{He}\left[\Phi(\sigma)\right] + XC_z^T C_z X & B_w \\ (*) & -\gamma^2 I \end{bmatrix}, \tag{35}$$

which can be converted by the Schur's complement [5] into

$$0 > \begin{bmatrix} -I & C_z X & 0 \\ (*) & \mathbf{He}\left[\Phi(\sigma)\right] & B_w \\ (*) & (*) & -\gamma^2 I \end{bmatrix}. \tag{36}$$

Therefore, condition (36) is guaranteed by (29) in light of $\Phi(\sigma) \in \mathbf{Co}(A_p X + B_u\overline{F}_p)$. □

Remark 8. In general, when investigating the output regulation problem of synchronous buck converters, we need to consider the dynamic behavior of some natural phenomena such as piecewise-constant load fluctuations and mismatch errors arising when generating the feedforward control. Thus, based on the framework of LPV control theory, this paper makes an attempt to impose such natural phenomena in the control design.

Table 1: Parameters of system (1)–(3).

Parameters	Value
Nominal input voltage v_I	12 V
Equilibrium point of $v_C(t)$	5 V
Inductance L	47 μH
Capacitance C	220 μF
Static drain to source resistance R_{DS}	30 mΩ
Equivalent series resistance of inductor R_{DCR}	100 mΩ
Equivalent series resistance of capacitor R_{ESR}	105 mΩ
Load resistance $R(t)$	5–10 Ω
Switching frequency	150 kHz

4. Simulation and Experimental Results

The parameters of the considered buck converter (1)-(3) are listed in Table 1. As shown in Table 1, the equilibrium point of $v_C(t)$ is given by $\overline{v}_C = 5$, and the lower and upper bounds of $R(t)$ are given by $R^- = 3$ and $R^+ = 20$, which leads to $f_{1,0} = 0.9662$, $f_{1,1} = 0.9948$, $f_{2,0} = 0.0.0497$, and $f_{2,1} = 0.0.3221$ from (17). As a result, system (15) can be represented as follows:

$$\begin{aligned} A_1 &= 10^2 \times \begin{bmatrix} -49.2445 & -205.5710 \\ 43.9174 & -2.2609 \end{bmatrix}, \\ A_2 &= 10^2 \times \begin{bmatrix} -49.8833 & -211.6548 \\ 45.2172 & -2.2609 \end{bmatrix}, \\ A_3 &= 10^2 \times \begin{bmatrix} -49.2445 & -205.5710 \\ 43.9174 & -14.6391 \end{bmatrix}, \\ A_4 &= 10^2 \times \begin{bmatrix} -49.8833 & -211.6548 \\ 45.2172 & -14.6391 \end{bmatrix}, \\ B_u^T &= B_w^T = 10^5 \times \begin{bmatrix} 2.5532 & 0 \end{bmatrix}, \\ C_z &= \begin{bmatrix} 0.1 & 0.1 \end{bmatrix}. \end{aligned} \tag{37}$$

For three LMI regions $\{\mathscr{D}_i\}_{i=1,2,3}$, Theorem 6 provides the corresponding control gains and the minimized $\mathscr{H}_\infty$ performances for (37), which are listed in Table 2. Figure 2 shows the behaviors of the output voltage $v_O(t)$, simulated by MATLAB (dot-line) and PSIM (solid-line), for the control gains corresponding to the LMI region $\mathscr{D}_2$. Here, to verify the effectiveness of the proposed approach, we consider the piecewise-constant load R_j that changes from 5 Ω to 10 Ω (see Figure 2(a)) and back to 5 Ω (see Figure 2(b)), where $\mathscr{T}_2 = 0.0025$ s is set for simulation. From Figure 2, it can be found that the transient responses obtained from MATLAB and PSIM simulations are approximately equal in view of the average mode, which means that the obtained LPV model (15) is valuable in investigating the regulation problem of synchronous buck converters. In particular, from the PSIM simulation result, we can see that the proposed control offers the short setting time 1 ms (less than $\mathscr{T}_2$ as mentioned in Remark 1), small overshoot 180 mV, and nearly zero steady state error even though there exist piecewise-constant load fluctuations in the synchronous buck converter.

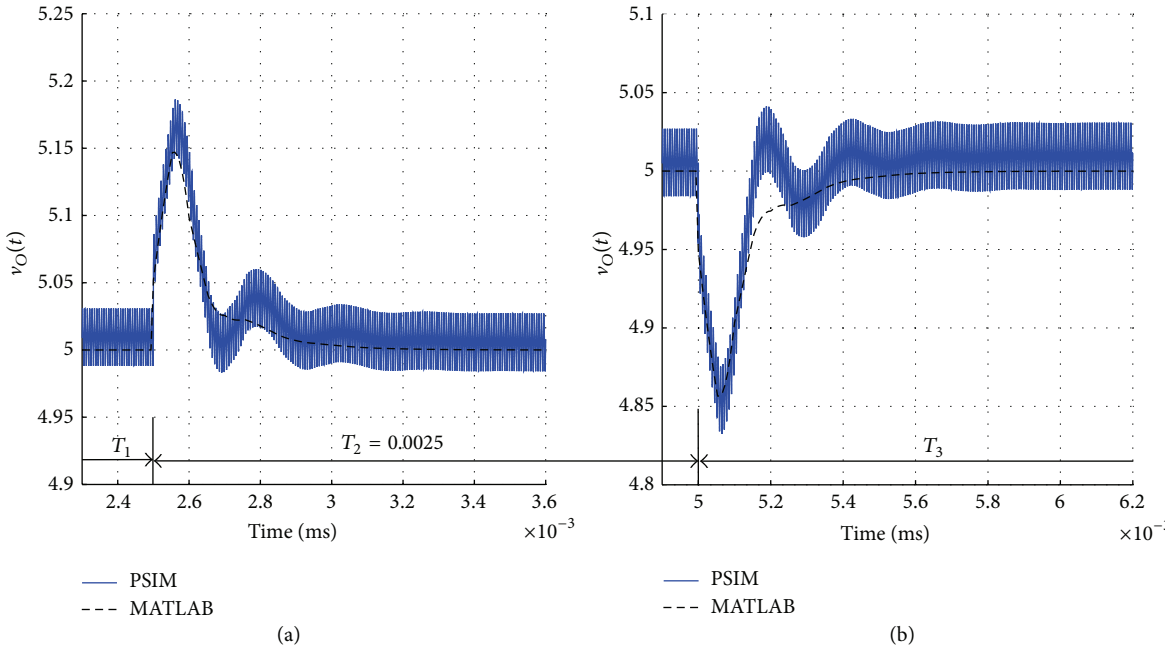

FIGURE 2: Simulation result. Output voltage $v_O(t)$ of the buck converter using the control gains for $\mathscr{D}_2$, where the load is changed: (a) from 5 Ω to 10 Ω at $t = 2.5 \times 10^{-3}$ and (b) from 10 Ω to 5 Ω at $t = 5 \times 10^{-3}$.

TABLE 2: $\mathscr{H}_\infty$ performance and control gains for each LMI region.

	α	r	θ	γ	Control gains
$\mathscr{D}_1$	11000	13000	$\pi/1000$	11.7050	$\begin{bmatrix} F_1 & F_2 \\ F_3 & F_4 \end{bmatrix} = \begin{bmatrix} -0.0738, -0.0422 & -0.0732, -0.0357 \\ -0.0704, -0.0216 & -0.0687, -0.0123 \end{bmatrix}$
$\mathscr{D}_2$	11000	15000	$\pi/1000$	4.5797	$\begin{bmatrix} F_1 & F_2 \\ F_3 & F_4 \end{bmatrix} = \begin{bmatrix} -0.0817, -0.0614 & -0.0813, -0.0550 \\ -0.0773, -0.0364 & -0.0715, -0.0290 \end{bmatrix}$
$\mathscr{D}_3$	11000	20000	$\pi/1000$	2.1914	$\begin{bmatrix} F_1 & F_2 \\ F_3 & F_4 \end{bmatrix} = \begin{bmatrix} -0.1012, -0.1094 & -0.1009, -0.1018 \\ -0.0986, -0.0868 & -0.0988, -0.0813 \end{bmatrix}$

Next, an experiment is additionally carried out to confirm the applicability of our approach verified through the simulation results. The parameters used herein are set the same as the ones listed in Table 1, and a dual N-channel MOSFET (FDS8949) and two current sense amplifiers (LMP8481) are used for the hardware implementation. Here, we need to tackle several problems concerning the measurement of the required output signals to construct the controller. First of all, the ringing problem arising from the used MOSFET should be addressed (1) by changing the Q-point factor that influences the setting time of v_O; and (2) by adding the RC snubber circuit placed between the low-side MOSFET and inductor. In what follows, the residual switching noises should be attenuated to exactly measure the values of $i_O(t)$, $i_L(t)$, and $v_O(t)$ with respect to the common ground. To do so, the power voltage v_I is thoroughly isolated from the applied voltage used for the operation of sensor units, which plays an important role in reducing such switching noises in the side of the sensor units. Finally, it is necessary to eliminate the undesirable effects of electromagnetic interference (EMI) that may be caused by the wrong PCB layout. In this sense, all net paths on the PCB board are designed as short as possible, and the top and bottom layers of the PCB board without inner layers are not assigned to draw the power and ground nets. Figure 3(a) shows the construction of our experimental bench, which consists of a prototype of buck converter (see Figure 3(b)), a dSPACE board, an oscilloscope, and an electronic loader. Here, data acquisition and real-time control system are implemented on the basis of dSPACE 1104 software and digital processor card, which have useful functions such as analog/digital converters (ADCs) and pulse-width modulation (PWM) built in TMS320F240 DSP. Figure 4(a) shows the output response $v_O(t)$ of the buck converter with R_j changing from 5 Ω to 10 Ω, from which we can observe that the maximum overshoot of $v_O(t)$ is approximately 180 mV and its setting time is less than 1.5 ms. In addition, Figure 4(b) shows the output response $v_O(t)$ of the buck converter with R_j changing back to 5 Ω, which illustrates that the maximum undershoot of $v_O(t)$ is approximately 180 mV and its setting time is less than 1.5 ms. That is, by making a comparison between Figures 2 and 4, we can see that this experiment achieves similar output transition performances to the ones

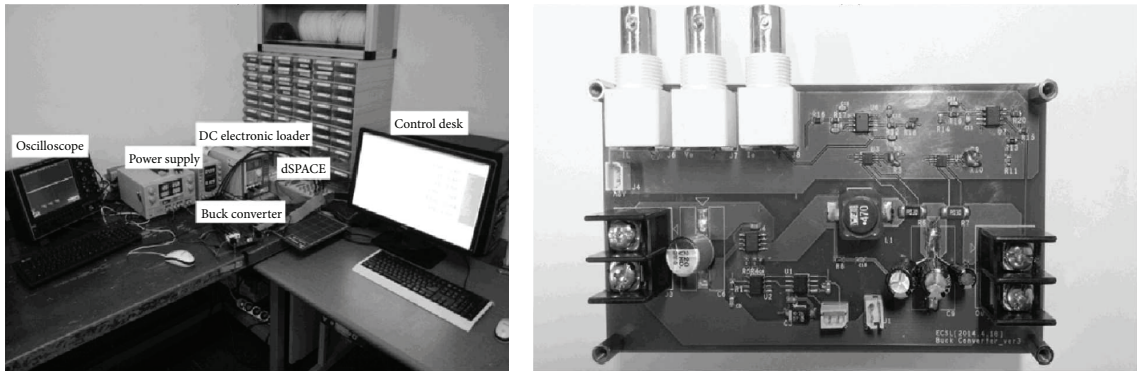

(a) (b)

Figure 3: (a) Experimental bench for testing the proposed approach and (b) experimental prototype of synchronous DC/DC buck converter.

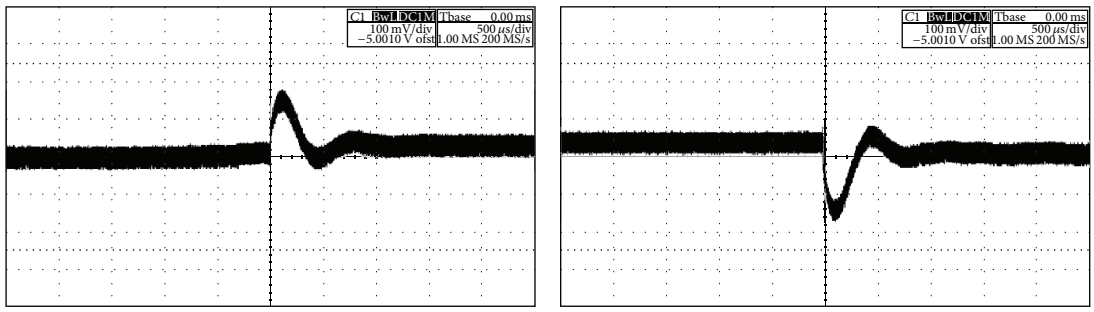

(a) (b)

Figure 4: Experiment result. Output voltage $v_O(t)$ of the buck converter using the control gains for $\mathscr{D}_2$, where the load is changed: (a) from 5 Ω to 10 Ω and (b) from 10 Ω to 5 Ω.

of the simulation results, which means that our approach can be practically applied to the output regulation problem of synchronous buck converters with load fluctuations.

5. Concluding Remarks

In this paper, we have shed some light on addressing the output regulation problem of synchronous buck converters with piecewise-constant load fluctuations via linear parameter varying (LPV) control scheme. Thus, based on the derived LPV model, an $\mathscr{H}_\infty$ stabilization condition is proposed such that (1) the mismatch error arising temporally in the feedforward control term can be attenuated and (2) the closed-loop poles can lie in the a prescribed LMI region. Finally, the validity of the proposed approach is verified through the simulation and experimental results.

Conflict of Interests

The authors declare that there is no conflict of interests regarding the publication of this paper.

Acknowledgment

This work was supported by the National Research Foundation of Korea Grant funded by the Korean Government (NRF-2012R1A1A1013687).

References

[1] C.-S. Chiu, "T-S fuzzy maximum power point tracking control of solar power generation systems," *IEEE Transactions on Energy Conversion*, vol. 25, no. 4, pp. 1123–1132, 2010.

[2] D. Saifia, M. Chadli, S. Labiod, and H. R. Karimi, "H_∞ fuzzy control of DC-DC converters with input constraint," *Mathematical Problems in Engineering*, vol. 2012, Article ID 973082, 18 pages, 2012.

[3] L.-F. Shi and W.-G. Jia, "Mode-selectable high-efficiency low-quiescent-current synchronous buck DC-DC converter," *IEEE Transactions on Industrial Electronics*, vol. 61, no. 5, pp. 2278–2285, 2014.

[4] R. Silva-Ortigoza, J. R. Garcia-Sanchez, and J. M. Alba-Martinez, "Two-stage control design of a buck converter/DC motor system without velocity measurements via a $\sum$ - Δ - modulator," *Mathematical Problems in Engineering*, vol. 2013, Article ID 929316, 11 pages, 2013.

[5] S. Boyd, L. E. Chauoi, E. Feron, and V. Balakrishan, *Linear Matrix Inequalities in System and Control Theory*, SIAM, Philadelphia, Pa, USA, 1994.

[6] K. Lian and C. Hong, "Current-sensorless flyback converters using integral T-S fuzzy approach," *International Journal of Fuzzy Systems*, vol. 15, no. 1, pp. 66–74, 2013.

[7] H. K. Lam and S. C. Tan, "Stability analysis of fuzzy-model-based control systems: application on regulation of switching *DC-DC* converter," *IET Control Theory & Applications*, vol. 3, no. 8, pp. 1093–1106, 2009.

[8] K.-Y. Lian, H.-W. Tu, and C.-W. Hong, "Current sensorless regulation for converters via integral fuzzy control," *IEICE Transactions on Electronics*, vol. 90, no. 2, pp. 507–514, 2007.

[9] K.-Y. Lian, J.-J. Liou, and C.-Y. Huang, "LMI-based integral fuzzy control of DC-DC converters," *IEEE Transactions on Fuzzy Systems*, vol. 14, no. 1, pp. 71–80, 2006.

[10] Y. Li and Z. Ji, "T-S modeling, simulation and control of the Buck converter," in *Proceedings of the 5th International Conference on Fuzzy Systems and Knowledge Discovery (FSKD '08)*, pp. 663–667, Schandong, China, October 2008.

[11] R. Nowakowski and N. Tang, "Efficiency of synchronous versus nonsynchronous buck converters," *Analog Applications Journal*, vol. 4, pp. 15–18, 2009.

[12] Y. Qiu, X. Chen, C. Zhong, and C. Qi, "Limiting integral loop digital control for DC-DC converters subject to changes in load current and source voltage," *IEEE Transactions on Industrial Informatics*, vol. 10, no. 2, pp. 1307–1316, 2014.

[13] G. Cimini, G. Ippoliti, S. Longhi, G. Orlando, and M. Pirro, "Synchronous buck converter control via robust periodic pole assignment," in *in Proceedings of European Control Conference (ECC '14)*, pp. 1921–1926, 2014.

[14] W.-R. Liou, M.-L. Yeh, and Y. L. Kuo, "A high efficiency dual-mode buck converter IC for portable applications," *IEEE Transactions on Power Electronics*, vol. 23, no. 2, pp. 667–677, 2008.

[15] Ó. Lucía, J. M. Burdio, L. A. Barragán, C. Carretero, and J. Acero, "Series resonant multiinverter with discontinuous-mode control for improved light-load operation," *IEEE Transactions on Industrial Electronics*, vol. 58, no. 11, pp. 5163–5171, 2011.

[16] X. Zhang and D. Maksimovic, "Multimode digital controller for synchronous buck converters operating over wide ranges of input voltages and load currents," *IEEE Transactions on Power Electronics*, vol. 25, no. 8, pp. 1958–1965, 2010.

[17] M. Qin and J. Xu, "Improved pulse regulation control technique for switching DC-DC converters operating in DCM," *IEEE Transactions on Industrial Electronics*, vol. 60, no. 5, pp. 1819–1830, 2013.

[18] S. Longhi and R. Zulli, "A robust periodic pole assignment algorithm," *IEEE Transactions on Automatic Control*, vol. 40, no. 5, pp. 890–894, 1995.

[19] S. H. Kim, "H_∞ output-feedback LPV control for systems with input saturation," *International Journal of Control, Automation and Systems*, vol. 10, no. 6, pp. 1267–1272, 2012.

[20] F. Wu and K. M. Grigoriadis, "LPV systems with parameter-varying time delays: analysis and control," *Automatica*, vol. 37, no. 2, pp. 221–229, 2001.

[21] X. Zhang and H. Zhu, "Robust stability and stabilization criteria for discrete singular time-delay LPV systems," *Asian Journal of Control*, vol. 14, no. 4, pp. 1084–1094, 2012.

[22] J. C. Doyle and G. Stein, "Multivariable feedback design: Concepts for a classical/modern synthesis," *IEEE Transactions on Automatic Control*, vol. 26, no. 1, pp. 4–16, 1981.

[23] B. A. Francis, *A Course in H_∞ Control Theory*, Lecture Notes in Control and Information Sciences, Springer, New York, NY, USA, 1987.

[24] M. Chilali and P. Gahinet, "H_∞ design with pole placement constraints: an LMI approach," *IEEE Transactions on Automatic Control*, vol. 41, no. 3, pp. 358–367, 1996.

[25] W. Assawinchaichote and S. K. Nguang, "Fuzzy H_∞ output feedback control design for singularly perturbed systems with pole placement constraints: an LMI approach," *IEEE Transactions on Fuzzy Systems*, vol. 14, no. 3, pp. 361–371, 2006.

[26] J. Sun and H. Grotstollen, "Averaged modeling of switching power converters: reformulation and theoretical basis," in *Proceedings of the 23rd Annual IEEE Power Electronics Sepecialists Conference (PESC '92)*, pp. 1165–1172, 1992.